Research Article

Norihan Abdullah*, Khalina Abdan, Muhammad Huzaifah Mohd Roslim, Mohd Nazren Radzuan, Ayu Rafiqah Shafi, and Lee Ching Hao

Properties of kenaf fiber-reinforced polyamide 6 composites

https://doi.org/10.1515/epoly-2022-8112
received December 29, 2022; accepted May 15, 2023

Abstract: Despite the increasing interest in polyamide-based composites, few studies on polyamide-based natural fiber composites have been conducted due to their high melting temperatures of polyamide 6 (PA6). In this study, kenaf fiber-reinforced polyamide 6 composites (KF/PA6) were successfully prepared and their properties were investigated. Thermogravimetric analysis demonstrated that the neat PA6 has higher thermal stability with higher melting temperatures of 426°C, respectively, than KF/PA6 composites. The results of the differential scanning calorimeter showed that the glass transition temperature (T_g) of KF/PA6 composites was slightly shifted to a higher temperature at 59°C than that of the neat PA6 at 45°C. The thermal and mechanical characteristics using dynamic mechanical analysis results showed that the storage and loss modulus of the neat PA6 were higher than those of KF/PA6 composites. The neat PA6 showed the maximum tensile strength of 48 MPa; however, the maximum tensile modulus was obtained at 10 wt% KF with 2,100 MPa. The flexural strength and modulus of the neat PA6 were 91 and 2,506 MPa, respectively, which were higher than those of KF/PA6 composites. The impact strength also deteriorated with the addition of KF, from 3.72 to 1.91 kJ·m^{-2}. Voids, fiber pulled-out, and agglomeration were observed in scanning electron microscope analysis on the tensile fractured surfaces.

Keywords: kenaf fiber, polyamide 6, composites, properties, mechanical

1 Introduction

Composites have been studied by many researchers in the way of utilization of lignocellulosic fillers, including natural fibers such as kenaf, flax, hemp, sisal, and jute (1,2). Use of the lignocellulosic fillers as raw materials has received a lot of attention as a replacement material to conventional mineral, glass, and carbon fibers (3). This is due to their beneficial characteristics, including competitive pricing, lightweight, excellent mechanical properties, ease of fiber modification, relative non-abrasiveness, biodegradability, process friendliness, good thermal, recyclability, and global availability (4–6). Furthermore, rising cost of petroleum and natural gas has increased pressure on finding alternate sources of energy for both engineering plastics (polyamides and polyesters) and commodity plastics (polyolefins such as polyethylene and polypropylene) (7). In addition, fossil products are predicted to run out within the next 40–60 years, forcing the focus on green and sustainable industries (8). As a result, there is a surge in the number of research on sustainable and environmentally friendly materials. As a part of environmentally friendly materials, there is growing interest in using natural fibers in composite plastics (9,10).

In recent decades, using natural fiber as a general filler or reinforcement has become a popular study topic (11,12). Kenaf fiber (*Hibiscus cannabinus*, L. family Malvaceae) is widely utilized because of its environmental and economic benefits with significant commercial values (13). The extremely low-price tag of kenaf raw materials has led to the production of inexpensive composites (14). Reportedly, kenaf fiber-reinforced polymer possesses unique physical and mechanical properties compared to other natural fibers (15). The tensile strength of kenaf fiber is higher

* **Corresponding author: Norihan Abdullah,** Laboratory of Biocomposite Technology, Institute of Tropical Forestry and Forest Products (INTROP), Universiti Putra Malaysia, 43400 Serdang, Selangor, Malaysia, e-mail: GS60118@student.upm.edu.my
Khalina Abdan, Ayu Rafiqah Shafi: Laboratory of Biocomposite Technology, Institute of Tropical Forestry and Forest Products (INTROP), Universiti Putra Malaysia, 43400 Serdang, Selangor, Malaysia
Muhammad Huzaifah Mohd Roslim: Department of Crop Science, Faculty of Agricultural and Forestry Sciences, Universiti Putra Malaysia Bintulu Campus, 97008 Bintulu, Sarawak, Malaysia
Mohd Nazren Radzuan: Department of Biological and Agricultural Engineering, Faculty of Engineering, Universiti Putra Malaysia, 43400 Serdang, Selangor, Malaysia
Lee Ching Hao: School of Engineering, Faculty of Innovation and Technology, Taylor's University, 47500 Subang Jaya, Selangor, Malaysia

than that of other natural fibers (with 930 MPa) (13). Kenaf fiber is a cellulosic source with lightweight, biodegradable, and highly specific mechanical properties without being abrasive during processing. Therefore, it can effectively reinforce various polymers (16,17). Kenaf fiber is widely used in the production of extruded, molded, and non-woven products due to its high flexural and tensile strength (19,20). Besides, the kenaf bast fibers possess striking mechanical properties that make them a replacement to glass fiber in polymer composites as reinforcing elements (21).

However, the term "natural fiber thermoplastic composites" mostly refers to polyolefin matrixes, regardless of the type of natural fibers (16). Therefore, in addition to polyolefin plastics, engineering plastics are now widely recognized as value-added materials due to their high quality and low density (22). As summarized by Ogunsona et al. (23), it is estimated that approximately 23% of polyamide is extruded into films and other extrusions for use in a variety of applications. The polyamide 6 (PA6) belongs to a significant group of engineering thermoplastics and possesses outstanding properties (24). These thermoplastics are competitive in terms of cost and performance, making them appealing to various industries (8). Furthermore, because of its hydrophilic nature, the use of PA6 in natural fiber composites has some advantages, such as higher mechanical properties compared to polyolefins. Recent research on lignocellulosic filler-reinforced PA6 has been extensively published (25–27). PA6's amide groups provide hydrogen bonds between polyamide chains, contributing to its excellent compatibility with natural fibers (28). This exceptional compatibility negates the need for a compatibilizer or a coupling agent. PA6 is a semi-crystalline engineering thermoplastic that competes with thermoset plastics due to its superior resistance to creep, stiffness, high melting temperatures, excellent barrier properties to oils and corrosive chemicals, as well as high tensile strength, modulus, and relative lightness (29,30). Then, the PA6 was also found to be easier to recycle than thermosets (31). Nowadays, recyclability is very advantageous due to increasing awareness of environmental concerns.

Despite academic and industrial interests in thermoplastic/natural fiber composites, there are very few reports of studies on natural fiber-reinforced engineering thermoplastic such as PA6 owing to processing challenges due to their higher melting point and thermal decomposition (32). Many studies have been attempted to upgrade the mechanical properties and stability as they have tremendous potentials as innovative alternative composite materials for residential and industrial applications. Thus, this article aims to lay the groundwork for future research on kenaf fiber and PA6-based engineering thermoplastic composites. Furthermore, this study also analyzes the effect of kenaf fiber reinforcement contents on chemical, thermal, mechanical, and morphological properties of PA6 composites.

2 Materials and methods

2.1 Materials

In this research, the main material used is PA6 polymer in pellet form, Grade CM1017, with a density of 1,130 kg·m^{-3}. The PA6 was purchased from Polycomposite Sdn. Bhd in Negeri Sembilan, and the kenaf fibers were purchased from the National Kenaf and Tobacco Board (LKTN), Kelantan. This study used kenaf fibers with a 40 mesh (400 μm) size.

2.2 Methods

The composites were extruded using a twin-screw extruder with a screw dimension (L & D) of 40:1 and a screw diameter of 30 mm. Before extrusion, both materials (PA6 and kenaf fibers) were dried in an oven for 24 h at 60°C, to prevent hydrolytic degradation during processing and to reduce the moisture content (<5%), respectively. Upon the fabrication of composites, the composition of the PA6 matrix and kenaf fiber reinforcements is shown in Table 1. All components were manually mixed before being fed into the main feeder of the extruder. The temperature profile of the extruder was divided into ten heating zones, ranging from 220 to 225°C, from the main feeder to the die. The extruded compounds were then granulated into pellets using a 2 mm Wiley mill, right after cooling in a water pool at 23 ± 2°C. To remove excess moisture, the composite pellets were dried in an oven for 24 h at 60°C. Using a laboratory hydraulic compression molding machine, the composite pellets were then fabricated into composite sheets with a dimension of 150 mm × 150 mm × 3 mm. The composites were pressed at 190°C for 10 min. Finally, the samples were cold-pressed at 15°C for 2 min. Then, the composite sheets were cut into

Table 1: Composition of kenaf fiber/PA6 composites

Samples	PA6 (wt%)	Kenaf fiber (wt%)
PA6	100	0
10% KF	90	10
20% KF	80	20
30% KF	70	30

specific standard sizes for further testing. The schematic of the kenaf fiber-reinforced polyamide 6 (KF/PA6) composite preparation process is depicted in Figure 1.

2.3 Characterization of kenaf fiber/PA6 composites

2.3.1 Fourier transform infrared spectroscopy (FTIR)

The FTIR spectra were recorded in the Perkin Elmer Spectrum 1,600 FT-IR Spectrometer in the wavenumber range of 500–4,000 cm^{-1}. The data were obtained using a 4 cm^{-1} resolution and 16 sample scans.

2.3.2 Thermal properties

2.3.2.1 Thermogravimetric analysis (TGA)

Thermal stability of the composites was measured in accordance with ASTM E1131 TA instrument Q500 (New Castle, DE, USA). In order to avoid sample oxidation, 5 to 6 mg of samples was kept in an open platinum pan with nitrogen flowing through it at a rate of 50 $mL{\cdot}min^{-1}$ at a temperature ranging from room temperature to 600°C by 10°C·min^{-1}. All results were recorded using TA universal analysis software.

2.3.2.2 Differential scanning calorimeter (DSC)

DSC is a common method for determining the thermo-physical properties of polymer composites. The DSC test was performed using TA instrument Q20 in accordance with ASTM D3418. Throughout the heating cycle, approximately 5 to 6 mg of sample was heated from room temperature to 250°C at a rate of 10°C·min^{-1}. Then, the data were reported by the TA universal analysis software. For each sample, glass transition temperature (T_g), melting temperature (T_m), crystallization temperature (T_c), enthalpy heat of melting (H_m), and crystallinity index (X_c) were determined. Eq. 1 is used to calculate the percentage of crystallinity for each curve. The theoretical heat fusion of PA6 at 100% crystalline ($\Delta H_{100\%}$) is 230 $J{\cdot}g^{-1}$ (33):

$$X_c = (\Delta H_m / \Delta H_{100\%}) \times 100 \quad (1)$$

2.3.2.3 Dynamic mechanical analysis (DMA)

DMA is a technique used to investigate viscoelastic behavior properties of polymers and composite materials. In accordance with ASTM D4065, a three-point bending mode was used under nitrogen protection using the TA instrument Q800. The test specimens were 63.5 mm × 12.7 mm × 3 mm in size (length × width × thickness). The frequencies used were 1 Hz at temperatures ranging from 30°C to 200°C, with a heating rate of 3 °C·min^{-1} and an amplitude of 15 m. The dynamic mechanical properties of composites, such as glass

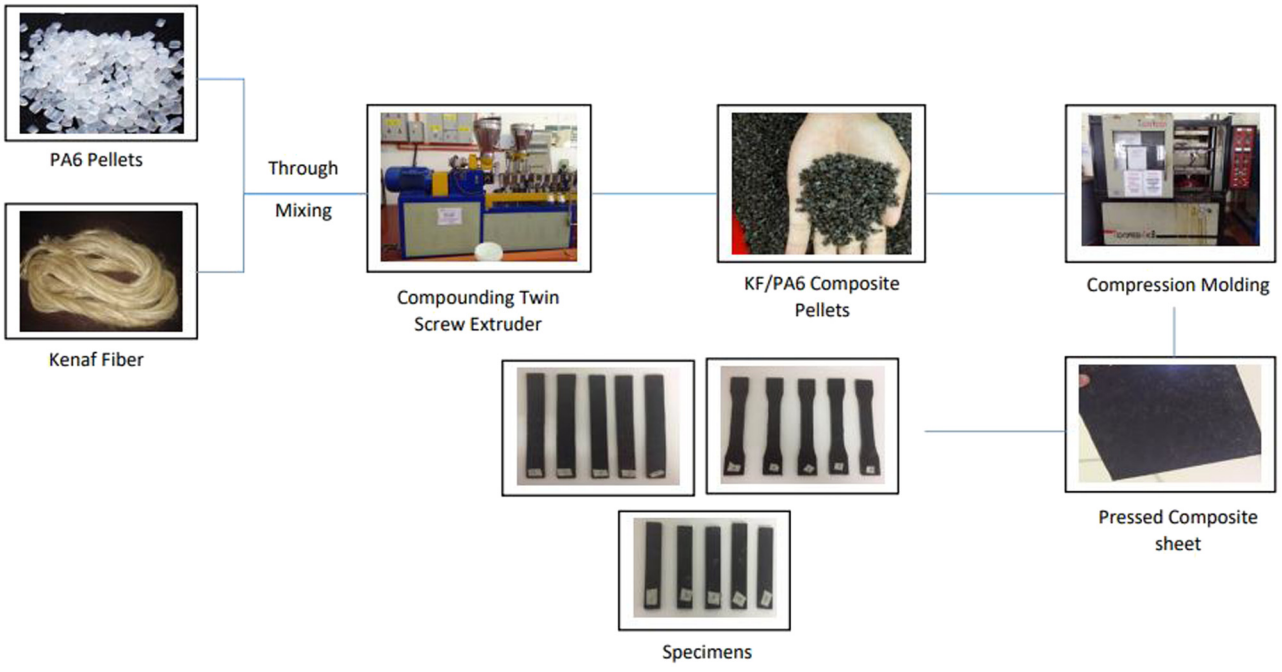

Figure 1: Schematic of the KF/PA6 composite preparation process.

transition temperature (T_g), storage modulus (E'), loss modulus (E''), and loss factor (tan δ), were investigated.

2.3.3 Mechanical properties

2.3.3.1 Tensile strength

The tensile strength of PA6/KF composites was measured using an Instron 5 kN machine. The PA6/KF composite sheets were die-cut into dog bone shapes in accordance with ASTM D638 (Type I) specifications. Prior to testing, the specimens were kept at 23°C ± 2°C and 50% ± 5% relative humidity. At room temperature, tests were performed with a strain rate of 2 mm·min^{-1} and a gauge length of 30 mm. A digital micrometer was used to measure the thickness and width of the narrow section for each sample. To establish statistical significance, five samples were repeated.

2.3.3.2 Flexural strength

Flexural strength was conducted in accordance with ASTM D790 using a 5 kN Instron Universal Testing machine. Prior to testing at a strain rate of 2 mm·min^{-1}, testing environment was regulated at 23°C ± 2°C and 50% ± 5% relative humidity. Using a band saw, flexural specimens were cut in size of 127 mm × 12.7 mm × 3 mm and tested flatwise on a support with a span-to-depth ratio of 16 (±). Five samples were examined to determine statistical significance.

2.3.3.3 Impact strength

In accordance with ASTM D256, the notched Izod impact strength was evaluated using a 0.5 J hammer. Using a band saw, the specimens measuring 63.5 mm × 12.7 mm × 3 mm were cut from the composite plates. An A-notch was then cut on the middle of specimen, with aids of dedicated notching machine that has a radius of curvature at the apex of 0.25 ± 0.05 mm. Before conducting the test, the pendulum-type hammer impact machine was calibrated to establish its accuracy. A fixture was used to position samples for clamping in the vise in order to minimize energy losses due to vibration. Five samples were evaluated for statistical significance.

2.3.4 Scanning electron microscopy (SEM)

The morphology of fractured samples from the tensile testing was determined using a Hitachi S-3400N SEM. To differentiate the matrix and the fiber, the samples were analyzed at an accelerated voltage of 15 kV. Prior to observation, the fractured surfaces were coated with a thin layer of gold using a sputter.

3 Results and discussion

3.1 FTIR

The FTIR spectra of the neat PA6 and KF/PA6 composites in the fingerprint region between 500 and 4,000 cm^{-1} range are illustrated in Figure 2. Those peaks represent the functional groups of PA 6 and kenaf fibers. However, the band locations and intensities did not vary significantly between the neat PA6 and KF/PA6 composites. The interaction of hydrogen bonding between the chains of one polymer and those of another in a composites is believed to change the IR spectra of composites if the materials are compatible.

The main FTIR bands are summarized in Table 2. The transition peaks occurring at 3,300–3,200 cm^{-1} as well as 3,000–2,800, 1,630–1,650, and the 1,550–1,510 cm^{-1} bands are depicted as the N–H and O–H stretching, CH_2 and CH_3 stretching, N–H stretching, amide I and amide II groups that are overlapped from PA6, respectively. These bands are closely linked to interfacial adhesion. It should be noted that as the kenaf fiber content increases, the wave numbers trend noticeably downward. The weaker bonding forces between carbon hydrogen, nitrogen hydrogen, and oxygen hydrogen are evidenced in the lower wave number (27). The difference in absorption intensity between kenaf fiber and PA6 confirms the network structure formed between kenaf fiber and PA6 (34). More specifically, it is

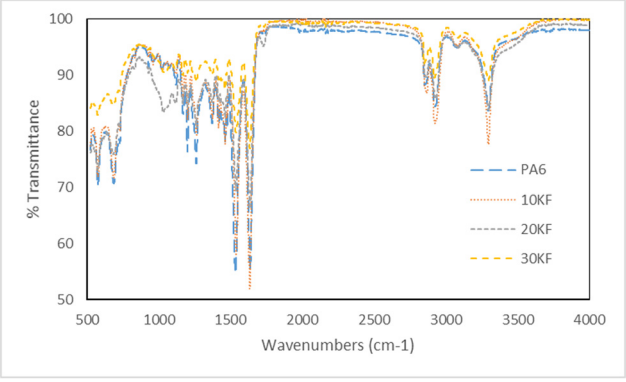

Figure 2: FTIR spectra of the neat PA6 and KF/PA6 composites.

observed the neat PA6, 10, and 20 wt% have a very similar intensity; meanwhile, 30 wt% is observed an increase in the intensity compared to neat PA6, 10, and 20 wt%.

3.2 Thermal properties

Figure 3 shows the TGA and differential thermogravimetric analysis curves for the neat PA6 and KF/PA6 composites. Thermogravimetry is a thermal analysis method that measures composite's mass changes, rate of thermal decomposition, and its thermal stability (35). The TGA curves show that KF/PA6 composites have three mass loss stages. At first stage, less than 3% of weight was lost at temperatures up to 200°C, and over 90% of total was lost between 200°C and 500°C, as second zone. The final or third zone was extended to temperature of 600°C in association with greater than 95 wt% of weight lost. The first initial loss is typically associated with a relatively small DTG peak and is attributed to the release of free water (moisture, humidity), as well as other volatiles, from the kenaf fibers, together with small molecular components, during sample storage and processing (27,36). Peaks in the DTG graphs at 250–450°C, 190–450°C, 160–450°C, and 150–450°C represented the decomposition of the hemicellulose, cellulose, and lignin components, respectively, in the kenaf fiber (37).

Table 3 summarizes the thermal stability of neat PA6 and KF/PA6 composites at various fiber contents. The composites thermally degraded at the kenaf fiber–PA6 matrix interface. As a result, the degradation temperatures of the neat PA6 and KF/PA6 composites are varied. The neat PA6 by itself has a maximum degradation temperature of 426°C. The addition of 10, 20, and 30 wt% kenaf fibers shows three gravimetric degradation peaks at 407°C, 401°C, and 404°C, respectively. Obviously, the degradation temperature of KF/PA6 composites was lower than that of the neat PA6. The decrement can be attributed to easily degradable components and the thermal damaging of the kenaf fiber-cross-linked structure (16,37). As kenaf fiber contents increased, the degradation-onset temperature (T_{onset}) fell. Degradation

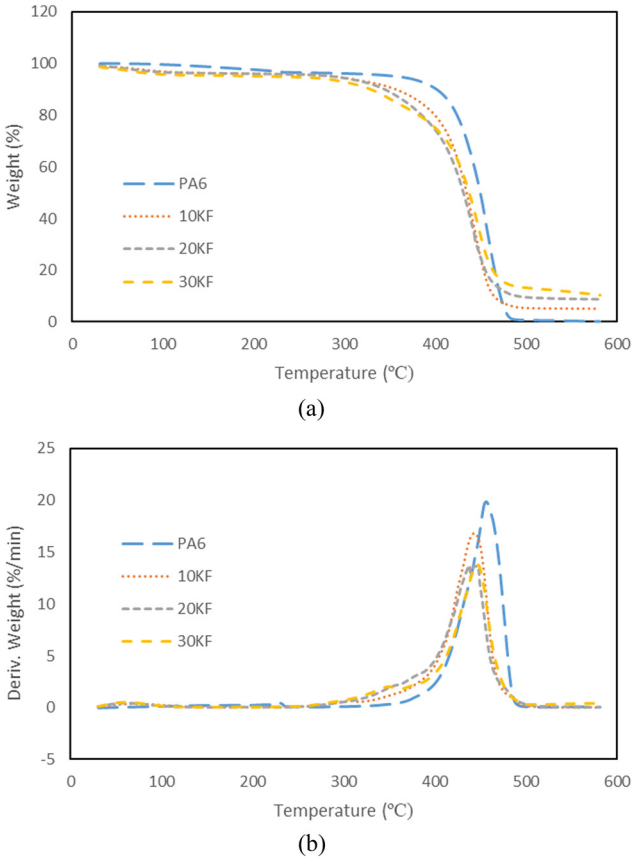

Figure 3: (a) TGA and (b) derivative TGA curves of the neat PA6 and KF/PA6 composites.

of the neat PA6 begins at 267°C, while 10, 20, and 30 wt% are 195°C, 162°C, and 152°C, respectively. This shows the fiber contents of the composites had significantly affected the thermal stability of composites. The low thermal stability of kenaf fibers resulted in a poor thermal stability of composites (36). This reduction is due to the thermal decomposition of the components in the kenaf fiber such as wax, pectin, and hemicellulose, followed by alpha cellulose and then lignin (16).

However, it was stated that in many of the works, the engineering thermoplastic improves the properties and enhances the thermal degradation of the composites due

Table 2: Main FTIR bands of neat PA6 and KF/PA6 composites

Peak location (cm^{-1})	Chemical structure	Motion	Neat PA6	10% KF	20% KF	30% KF
3,200–3,400	O–H and N–H	Stretching	3,296	3,296	32,96	3,295
3,000–2,800	CH_2 and CH_3	Stretching	2,872–2,922	2,866–2,921	2,861–2,921	2,849–2,918
1,630–1,650	N–H	Stretching	1,636	1,633	1,635	1,633
1,550–1,510	Amide I and amide II	Combined motion	1,534	1,534	1,533	1,533

Table 3: TGA results of neat PA6 and KF/PA6 composites

Sample	T_{onset} (°C)	T_{endset} (°C)	$T_{decomposed}$ (°C)	Weight loss (%)	Residue at 600°C (%)
PA6	267	456	426	96	0.21
10% KF	195	443	407	91	5.14
20% KF	162	444	401	87	8.77
30% KF	152	444	404	85	10.39

to higher degradation temperature compared to other polyolefin matrixes (17,18). At 600°C, the residue of KF/PA6 composites increased as the kenaf fiber content increased. This indicates that kenaf fiber is primarily responsible for the increase in residues. It contains more lignin, which aids in char formation and structural integrity (39). Besides, the kenaf fiber is wrapped in the PA6 matrix, thus preventing the escape of volatiles produced during the thermal decomposition and finally leading to higher residue formation.

DSC is a method of thermal analysis that measures the temperature and heat flow of a material change as a function of time and temperature (40). The DSC curves of the neat PA6 and KF/PA6 composites are shown in Figure 4. Table 4 presents the T_c, T_m, and crystallinity of the neat PA6 and KF/PA6 composites. Composites reinforced with 20 wt% kenaf fibers have a higher T_c than the pure PA6 polymer.

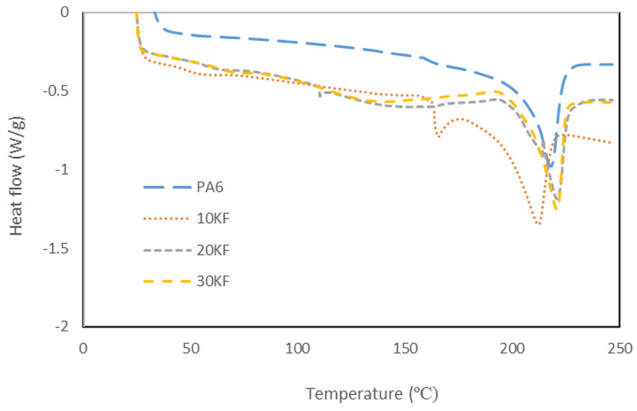

Figure 4: DSC thermograms of the neat PA6 and KF/PA6 composites.

Nucleating effects of the kenaf fiber are responsible for this improvement because it quickens the rate at which crystals form (41). In this way, KF/PA6 composites accelerate the crystallization of PA6 compared to homogeneous crystallization itself. However, 30 wt% has lower T_c compared to 20 wt% because the kenaf fiber prevents the PA6 molecular chains from migrating and diffusing in the composites, which caused a negative effect on polymer crystallization, thus resulting in a reduction in T_c (41,42).

On the other side, the T_m of KF/PA6 composites ranged from 217°C to 220°C, which showing insignificant effects. These results indicated that the addition of fiber contents did not affect the presence of the PA6 crystallites (42). Yet, with a reduction in the mobility of PA6 polymer chains, there was an upward shift in the glass transition temperature (T_g) to a higher level. In the KF/PA6 composite system, the kenaf fiber particles restrict the PA6 molecular chain movements, and a large amount of energy and free volume are required (43). Therefore, T_g increases with the increase in the kenaf fiber contents. The increment of kenaf fiber contents is also associated with a decrease in crystallization enthalpies (ΔH_c). Similar result was reported by Kiziltas et al. (38), for KF/PA6 composites. It is well known that crystallinity is a measure of the crystalline region's concentration. The higher the percentage of kenaf fibers, the less crystalline the composites became (37,44). The neat PA6 polymer possesses higher crystallinity (X_c) compared to the KF/PA6 composites. This could be interpreted as a strong interfacial interaction between matrix and fibers, thus reducing the degree of regularity of the polymer chains, limiting the movement of PA6 molecular chains, and causing a decrease in crystallinity (44). Besides, although the kenaf

Table 4: DSC results of neat PA6 and KF/PA6 composites

Sample	Melting temperature, T_m (°C)	Crystallization temperature, T_c (°C)	Glass transition, T_g (°C)	Melting enthalpy, ΔH_m (J·g^{-1})	Crystallinity index, X_c (%)
PA6	217	205	45	76	33
10% KF	212	206	46	57	25
20% KF	220	211	56	51	22
30% KF	220	207	59	53	23

fiber provides nucleating sites for PA6 crystallization, it may also act as a barrier to crystal growth (45). The fiber contents have no significant effects on the T_c and T_m of composites, but it does affect the crystallinity index.

DMA was used to investigate the thermo-mechanical properties of the neat PA6 and KF/PA6 composites. The variations in storage modulus (E'), loss modulus (E''), and tan delta (tan δ) for the neat PA6 and KF/PA6 composites as a function of temperature are shown in Figure 5(a)–(c), respectively. Due to the reduced viscosity and increased polymer chain mobility, the E' curves at higher temperatures showed a significant decrease in E' (13). When comparing the various composites, it was discovered that as the kenaf fiber loading increases, the value of E' decreases as a result of losing stiffness. However, the 10 wt% kenaf fibers composite had the highest E' and this may be due to better stress transfer at the fiber interface. Loss modulus values for the KF/PA6 composites were observed to decrease with increasing fiber loading, similar to storage modulus. The loss modulus of the composite decreased from 100 MPa for the neat PA6 to 97, 65, and 44 MPa for 10, 20, and 30 wt% kenaf fiber contents, respectively. The tan δ peak values of KF/PA6 composites decreased from 0.11 for 10 wt% to 0.07 for 20 and 30 wt% kenaf fiber, respectively. Besides, the neat PA6 had a tan δ max peak temperature of 50°C, whereas the KF/PA6 had values ranging from 50°C to 62°C, indicating that the peaks had shifted to a higher temperature. The tan δ peak is the temperature that corresponds to the Tg, and the increase in the tan δ of KF/PA6 composites was found synchronized with the DSC results. The peaks had been shifting to a higher temperature as the kenaf fiber contents increased, possibly because the kenaf fiber restricted the PA6 melt mobility, which reduced the damping of the composite material (46). The tan δ values also decreased as the kenaf fiber content increased (29). However, the 10 wt% kenaf fiber shows better damping property as compared to the neat PA6.

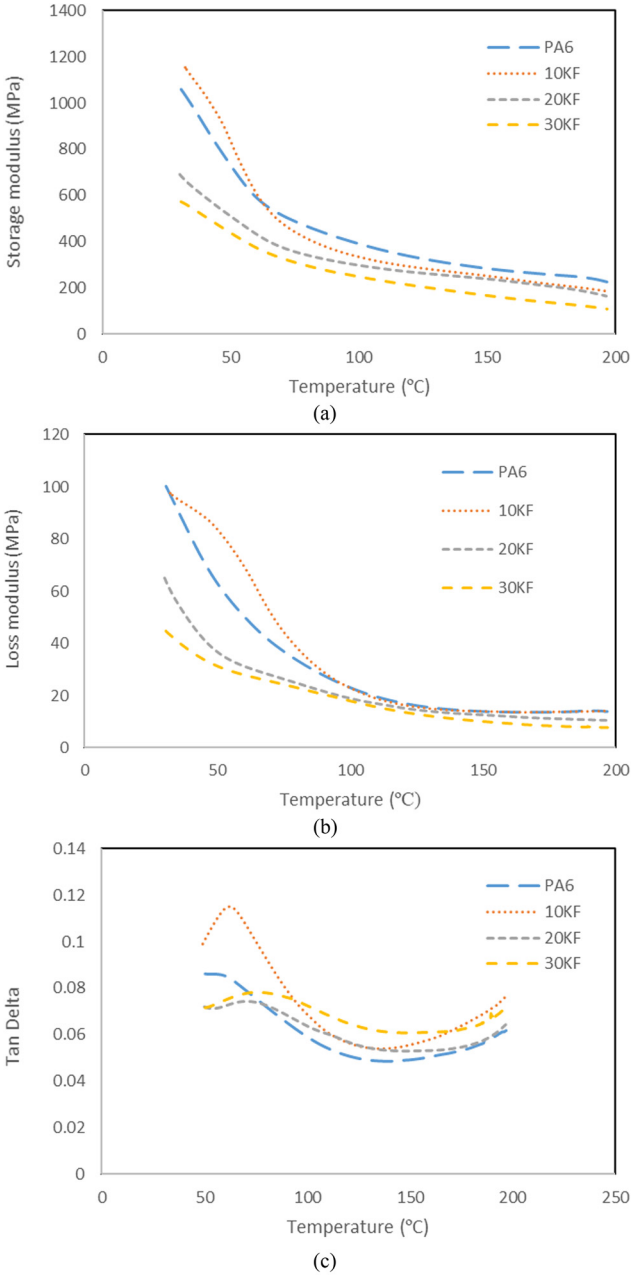

Figure 5: DMA curves: (a) storage modulus (E'), (b) loss modulus (E''), and (c) tan delta (tan δ) of the neat PA6 and KF/PA6 composites.

3.3 Mechanical properties

Figure 6 shows the tensile strength and Young's modulus for the neat PA6 and KF/PA6 composites. There is an enormous difference in tensile strength between the neat PA6 and its composites, as shown in Figure 5. No increment

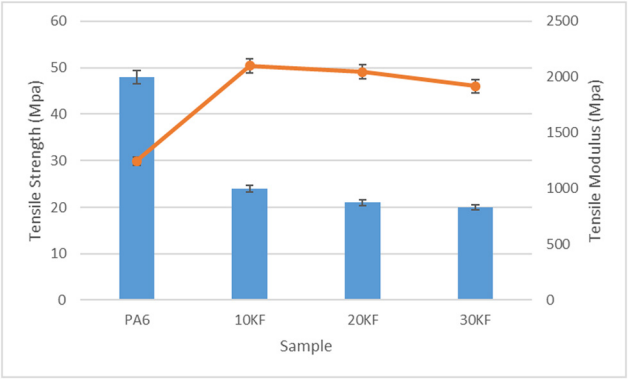

Figure 6: Tensile strength and tensile modulus of the neat PA6 and PA6/KF composites.

effects were observed by kenaf fiber reinforcements in the tensile strength of the PA6 composites. This is due to the ineffective load transfer between kenaf fiber reinforcement and its matrix (47). From the obtained results and considering the variations in fiber contents, it shows that the fiber–matrix interactions play a major role in the mechanical performance of composites. Notably, it was difficult for PA6 and its reinforcements to interact due to the presence of lignin in the fibers, which likely resulted in a low interfacial shear stress (25).

On the other hand, the tensile strength of the composites showed that there is no significant difference between the 10, 20, and 30 wt% kenaf fiber, respectively. As the kenaf fiber increases, the strength of the KF/PA6 composites decreases. It is shown that the maximum tensile strength is obtained at 10 wt% kenaf fiber with 24 MPa compared to 20 and 30 wt% with 21 and 20 MPa, respectively. These outcomes could be explained by the debonding of the kenaf fibers from the PA6 matrix and the pulling-out of fibers (48). Besides, 20 and 30 wt% kenaf loading specimens demonstrated approximately 13.19% and 14.42% lower tensile strength than 10 wt% KF/PA6 composite, respectively. Some studies on PA6 cellulose composites revealed an improvement in mechanical properties at lower cellulose concentrations, but a decrease in tensile properties at higher concentrations (49). When there are more fibers per unit volume, the polymer has a harder time penetrating the voids between the fillers. This leads to poor wettability by the matrix, low interaction between the fibers and the PA6 matrix, agglomeration, embrittlement of the overall sample, and hindered stress transfer through the interface (50). The dog bone-shaped specimens and the brittle fracture surface of the specimens after the tensile testing are shown in Figure 7a and b, which will be discussed in the SEM section.

The results show that 10, 20, and 30 wt% kenaf fiber reinforcements have higher tensile modulus compared to the neat PA6. It is shown that the maximum tensile modulus is obtained at 10 wt% kenaf fiber with 2,100 MPa compared to that of neat PA6, 20, and 30 wt% with 1,247, 2,046, and 1,918 MPa, respectively. The kenaf fiber exhibited a strong enhancement effect on PA6. The results of the tensile modulus showed a significant increment for 10, 20, and 30 wt% kenaf fiber, which showed a 40.61%, 39%, and 35%, respectively, over the neat PA6. It can be noted that the addition of kenaf fiber increases the tensile modulus. This finding was primarily attributed to the interfacial adhesion and flow of PA6 within kenaf fibers (51). This result supports the finding by Ozen et al. (8), who found that since the PA6 and its reinforcement adhered so well to one another, the tensile modulus of the composite material increased. A composite system strengthened by kenaf fiber with a high modulus can better withstand the applied stress (46). The addition of kenaf fibers to the matrix of PA6 prevents PA6 from deforming elastically, producing composites with a high tensile modulus of elasticity. Besides, the KF/PA6 composites are made of a low-stiffness PA6 matrix and a high-stiffness kenaf fiber filler. Consequently, the stiffness increases as fiber volume increases (52).

The effects of different kenaf fiber contents on the flexural strength and modulus of elasticity are shown in Figure 8. When compared to the neat PA6, the flexural strength and modulus of KF/PA6 composites were both reduced by the addition of kenaf fiber. The flexural strength and modulus of the neat PA6 were 91 and 2,506 MPa, respectively. In comparison with the neat PA6, the flexural strength of KF/PA6 composites with 10, 20, and 30 wt% kenaf fiber contents decreased by 47%, 48%, and 60%, respectively, while the flexural modulus decreased by 39%, 46%, and 52%, respectively. This could be because weak interfacial bonds are

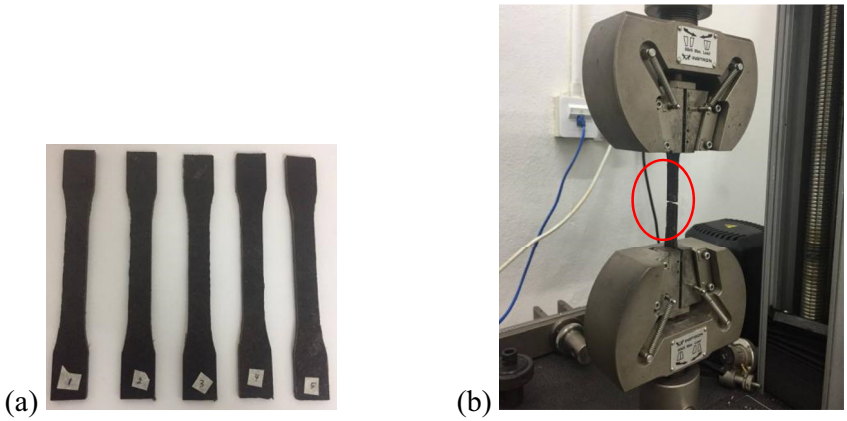

Figure 7: (a) The dog bone-shaped specimens and (b) brittle fracture surface of the specimens after the tensile testing.

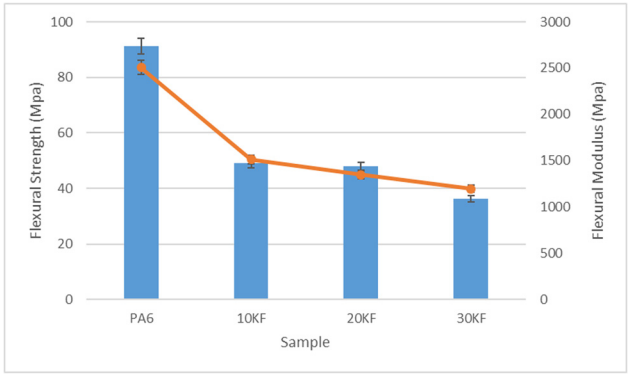

Figure 8: Flexural strength and flexural modulus of the neat PA6 and PA6/KF composites.

made between the kenaf fiber and the PA6 matrix, even though the hydrogen bonds are formed between the hydroxyl of kenaf fibers and the amide groups of PA6 (25). Moreover, the kenaf fiber impeded the mobility of PA6 chains and destructed the PA 6's original toughening effects (53). The connection between kenaf fiber and PA6 got weaker, which means that in this study, kenaf fibers act as fillers instead of reinforcing fibers. As kenaf fiber contents increased, the flexural strength and modulus of KF/PA6 composites decreased. This decreasing trend of flexural strength is likely due to the tensile strength, and the less kenaf fiber content at 10 wt% showed the less damage compared to that at 20 and 30 wt%. Besides, the 10 wt% kenaf fiber has better deformation resistance than the other KF/PA6 composites. Kenaf fiber in the PA6 matrix also increases its rigidity when compared to 20 and 30 wt% kenaf fiber. The weakening of the PA6 coating on kenaf fiber and poor dispersibility of kenaf fiber led to failure at relatively low loads caused by agglomerated fragile points and stress concentration (46). This may also be the reason why the elongation rate and break strain decreased as the kenaf fiber content rose. High levels of kenaf fiber would encourage friction heat, which would cause the fiber to continue to deteriorate and lose strength.

Figure 9 shows the notched impact strength of the neat PA6 and PA6/KF composites. For impact strength, the values were measured in the range of 3.72 to 1.91 kJ·m^{-2}. The addition of kenaf fiber reduced the notched impact strength of PA6 and the downward trend became more obvious as the kenaf fiber content rose. The impact strength was significantly affected by the fiber loading. At kenaf fiber contents of 10, 20, and 30 wt%, the notched impact strengths are 2.37, 2.23, and 1.71 kJ·m^{-2}, respectively. These values are 36.29%, 40.05%, and 54.03% lower than the neat PA6 primarily due to the high rigidity of high-temperature arbonized kenaf fiber (46). Besides, the PA6 molecular chain's flexibility and mobility were both reduced by the presence of kenaf fiber and the plastic deformation of composites was limited, and therefore, less energy loss was observed. The addition of kenaf fiber to PA6 made the composite more fragile and reduced its capacity to absorb energy. The ductility of composites is thought to be the cause of their relatively low tensile and flexural modulus. Thus, the resistance of composites to impact damage subsequently weakened and their toughness decreased (24). The PA6 molecular chain, in particular, became increasingly constrained as the kenaf fiber contents increased, and a further reduction in its capacity to withstand impact load led to a significant weakening of the material's toughness. Others have reported a decrease in impact strength values associated with the presence of lignocellulosic filler (37). Intriguingly, the 10 wt% notched impact strength was greater than that of other PA6/KF composites. This is most likely due to the fact that 10 wt% had the highest interfacial bonding strength and the highest interface compatibility at this ratio compared to 20 and 30 wt%.

3.4 SEM

Under an electron microscope, the morphology of the neat PA6 and KF/PA6 composites was examined. Figure 9 shows the SEM micrographs of the tensile fractured surfaces to study the interfacial bonding between the neat PA6 and KF/PA6 composite samples. Figure 10(a) shows the fracture surface of neat PA6 that exhibited a relatively flat fracture surface, while kenaf fiber was found in the composites as shown in Figure 10(b)–(d). The roughness of the surface, along with undulations and local protrusions, increased after the addition of kenaf fiber particles, primarily due to the action of external force (46). Besides, the PA6 was pulled and held together by the kenaf fiber particles although during the fracturing process, the PA6 matrix was damaged. As a result, the PA6 matrix distributed its stress to the kenaf fiber particles. This resulted in a greater

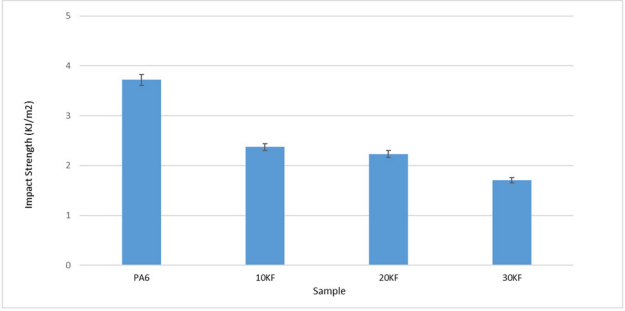

Figure 9: Impact strength of the neat PA6 and PA6/KF composites.

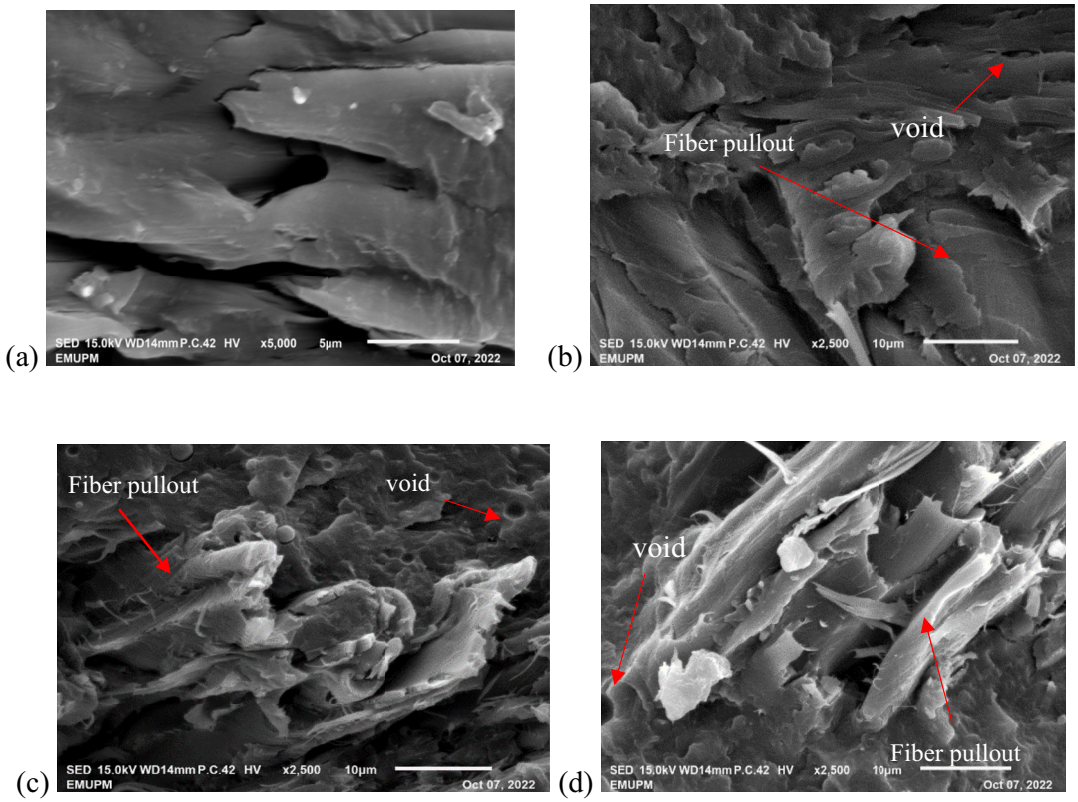

Figure 10: SEM images of tensile fracture morphology: (a) neat PA6, (b) 10 wt%, (c) 20 wt%, and (d) 30 wt%.

number of undulating surfaces. The KF/PA6 composites showed surface distortion characteristic and ductile deformation increased after the addition of kenaf fiber particles (43).

When compared to the neat PA6, the KF/PA6 composites have an interconnecting network structure that is conducive to the tensile modulus. In KF/PA6 composites, the matrix polymer prominently covers the kenaf fiber, exhibiting adhesion of the fiber to the matrix. Additionally, a broken fiber, debonding, and crack can be seen on the structure of the matrix, indicating that the fiber and matrix's interface caused both phases to fail during the fracture process (8). Besides, the morphology of the KF/PA6 composites had an impact on their tensile strength as well. Figure 10(b)–(d) also reveals the thermal degradation of the kenaf fiber that causes voids in KF/PA6 composites, which has a negative effect on the properties of composites (27). It is possible that the fibers slipped out of the PA6 matrix, causing these voids. Furthermore, during compounding, the fiber agglomeration may occur during the compounding process, which will result in a reduction in the effective surface area of the composite (54). As the percentage of kenaf fiber in the composites increased, the particles of kenaf fiber were dispersed throughout the PA6 matrix and became denser; therefore, the particle bonding generated agglomeration and few pores (46). Besides, as the kenaf fiber contents increased, the voids between fibers and matrix became larger and more obvious due to matrix cracking, pulled-out fibers, and discontinuities at the fiber–matrix interfaces, indicating a weakening of the fiber–matrix interface, resulting in a decrease in tensile strength (25).

4 Conclusions

In this study, extrusion was used as the method to fabricate KF/PA6 composites with different kenaf fiber contents. The chemical, thermal, mechanical, and morphological properties of different kenaf fiber contents were discussed. An increase in kenaf fiber loadings had reduced the thermal stability of the material. TGA demonstrated that the neat PA6 has higher thermal stability with higher initial and final decomposition temperatures of 266°C and 456°C, respectively, than the KF/PA6 composites by exhibiting a decrease in the values of 152°C and 144°C, respectively. The results of the DSC showed that the glass transition temperature (T_g) of KF/PA6 composites was slightly shifted to a higher temperature at 59°C than that of the neat PA6 at 45°C, which affected the crystallization behavior of the composites. The

thermal–mechanical characteristics from DMA results showed that the storage and loss modulus of the neat PA6 are 1,059 and 100 MPa, respectively, which indicates that KF/PA6 composites deteriorated by 572 and 44 MPa, respectively. The tensile and flexural properties of KF/PA6 composites, as well as their corresponding Young's modulus, were lower than those of the neat PA6. The maximum tensile modulus is obtained at 10 wt% kenaf fiber with 2,100 MPa compared to that of the neat PA6; however, the neat PA6 showed the maximum tensile strength of 48 MPa. The flexural strength and modulus of the neat PA6 were 91 and 2,506 MPa, respectively. In comparison with the neat PA6, the flexural strength of KF/PA6 composites decreased by 47%, 48%, and 60%, respectively, while the flexural modulus decreased by 39%, 46%, and 52%, respectively. The impact strength also deteriorated with the addition of kenaf fiber, from 3.72 to 1.91 $kJ \cdot m^{-2.}$ These values are 36.29%, 40.05%, and 54.03% lower than that of the neat PA6. Also, the observation of the SEM micrographs showed that there were few voids, agglomeration, and pull-out of fibers within the PA6 matrix. This indicates lower mechanical properties, implying weak interfacial bonding between the fibers and the matrix. From the study, among the KF/PA6 composites, it can be said that 10 wt% is the optimum fiber loading because it exhibited better properties compared to 20 and 30 wt%.

Acknowledgements: The authors would like to thank Universiti Putra Malaysia for the financial support provided by the Universiti Putra Malaysia under Putra Grant Berimpak scheme (GPB/2020/9691300). The authors would like to acknowledge the contributions of Farah Nora Aznieta Abdul Aziz (Department of Civil Engineering, Faculty of Engineering, UPM), Mohamed Thariq Hameed Sultan (Laboratory of Biocomposite Technology, Institute of Tropical Forestry and Forest Products, UPM), and Hyung-joon Kim (Department of Materials Science and Engineering, Universiti of Seoul, Korea) for their support throughout the research process.

Funding information: This study was funded by Putra Grant Berimpak, grant number 9691300 (GPB/2020/9691300).

Author contributions: Norihan Abdullah: draft manuscript preparation, analysis and interpretation of results, manuscript writing, review, and editing; Khalina Abdan: resources, study conception and design, review, and editing; Muhammad Huzaifah Mohd Roslim: interpretation of results, review, and editing; Mohd Nazren Radzuan: interpretation of results, review, and editing; Ayu Rafiqah Syafi: interpretation of results, review, and editing; Lee Ching Hao: interpretation of results, review, and editing.

Conflict of interest: The authors state no conflict of interest.

Data availability statement: The raw/processed data required to reproduce these findings cannot be shared at this time as the data also forms part of ongoing study.

References

(1) Mochane MJ, Mokhena TC, Mokhothu TH, Mtibe A, Sadiku ER, Ray SS. Recent progress on natural fiber hybrid composites for advanced applications: a review. Express Polym Lett. 2019;13(2):159–98.
(2) Sanjay MR, Madhu P, Jawaid M, Senthamaraikannan P, Senthil S, Pradeep S. Characterization and properties of natural fiber polymer composites: A comprehensive review. J Clean Prod. 2018;172:566–81. doi: 10.1016/j.jclepro.10.101.
(3) Sanjay MR, Madhu P, Jawaid M, Senthamaraikannan P, Senthil S, Pradeep S. Characterization and properties of natural fiber polymer composites: a comprehensive review. J Clean Prod. 2017;172:566–81. doi: 10.1016/j.jclepro.2017.10.101.
(4) Atiqah A, Chandrasekar M, Senthil Muthu Kumar T, Senthilkumar K, Ansari MNM. Characterization and interface of natural and synthetic hybrid composites. Encycl Renew Sustain Mater. 2020;4:389–400. doi: 10.1016/b978-0-12-803581-8.10805-7.
(5) Devnani GL, Sinha S. Effect of nanofillers on the properties of natural fiber reinforced polymer composites. Mater Today: Proc. 2019;18:647–54. doi: 10.1016/j.matpr.2019.06.460.
(6) Karthi N, Kumaresan K, Sathish S, Gokulkumar S, Prabhu L, Vigneshkumar N. An overview: Natural fiber reinforced hybrid composites, chemical treatments and application areas. Mater Today: Proc. 2019;27:2828–34. doi: 10.1016/j.matpr.2020.01.011.
(7) Yashas Gowda TG, Sanjay MR, Subrahmanya Bhat K, Madhu P, Senthamaraikannan P, Yogesha B. Polymer matrix-natural fiber composites: An overview. Cogent Eng. 2018;5(1):1446667. doi: 10.1080/23311916.2018.1446667.
(8) Ozen E, Kiziltas A, Kiziltas EE, Gardner DJ. Natural fiber blend — nylon 6 composites. Polym Compos. 2013;34(4):544–53. doi: 10.1002/pc.
(9) Srinivas K, Lakshumu Naidu A, Raju Bahubalendruni MVA. A review on chemical and mechanical properties of natural fiber reinforced polymer composites. Int J Perform Eng. 2017;13(2):189–200. doi: 10.23940/ijpe.17.02.p8.189200.
(10) Thyavihalli Girijappa YG, Mavinkere Rangappa S, Parameswaranpillai J, Siengchin S. Natural fibers as sustainable and renewable resource for development of eco-friendly composites: a comprehensive review. Front Mater. 2019;6:1–14. doi: 10.3389/fmats.2019.00226.
(11) Mohammed AA, Bachtiar D, Siregar JP, Rejab MRM. Effect of sodium hydroxide on the tensile properties of sugar palm fibre reinforced thermoplastic polyurethane composites. J Mech Eng Sci. 2016;10(1):1765–77. doi: 10.15282/jmes.10.1.2016.2.0170.
(12) Sahu P, Gupta MK. A review on the properties of natural fibres and its bio-composites: effect of alkali treatment. Proc Inst Mech Engineers, Part L: J Mater: Des Appl. 2020;234(1):198–217. doi: 10.1177/1464420719875163.
(13) Mlik YBen, Jaouadi M, Rezig S, Khoffi F, Slah M, Durand B. Kenaf fibre-reinforced polyester composites: Flexural characterization

and statistical analysis. J Text Inst. 2017;109(6):713–22. doi: 10.1080/00405000.2017.1365580.
(14) Sreenivas HT, Krishnamurthy N, Arpitha GR. A comprehensive review on light weight kenaf fiber for automobiles. Int J Lightweight Mater Manuf. 2020;3(4):328–37. doi: 10.1016/j.ijlmm.2020.05.003.
(15) Fauzi FA, Ghazalli Z, Siregar JP. Effect of various kenaf fiber content on the mechanical properties of composites. J Mech Eng Sci. 2016;10(3):2226–33. doi: 10.15282/jmes.10.3.2016.2.0208.
(16) Kamarudin SH, Abdullah LC, Aung MM, Ratnam CT. Thermal and structural analysis of epoxidized jatropha oil and alkaline treated kenaf fiber reinforced poly(Lactic acid) biocomposites. Polymers. 2020;12(11):1–21. doi: 10.3390/polym12112604.
(17) Ramesh M, Rajeshkumar LN, Srinivasan N, Kumar DV, Balaji D. Influence of filler material on properties of fiber-reinforced polymer composites: a review. e-Polymers. 2022;22:898–916. doi: 10.1515/epoly-2022-0080.
(18) Radzuan NAM, Tholibon D, Sulong AB, Muhamad N, Che Haron CH. Effects of high-temperature exposure on the mechanical properties of Kenaf composites. Polymers. 2020;12:1643. doi: 10.3390/polym12081643.
(19) Keya KN, Kona NA, Koly FA, Maraz KM, Islam MN, Khan RA. Natural fiber reinforced polymer composites: history, types, advantages, and applications. Mater Eng Res. 2019;1(2):69–87. doi: 10.25082/mer.2019.02.006.
(20) Yusuff I, Sarifuddin N, Ali AM. A review on kenaf fiber hybrid composites: Mechanical properties, potentials, and challenges in engineering applications. Prog Rubber Plast Recycling Technol. 2021;37(1):66–83. doi: 10.1177/1477760620953438.
(21) Verma R, Shukla M. Characterization of mechanical properties of short Kenaf fiber-HDPE green composites. Mater Today: Proc. 2018;5(2):3257–64. doi: 10.1016/j.matpr.2017.11.567.
(22) Elsabbagh A, Steuernagel L, Ring J. Natural fibre/PA6 composites with flame retardance properties: extrusion and characterisation. Compos Part B: Eng. 2017;108:325–33. doi: 10.1016/j.compositesb.2016.10.012.
(23) Ogunsona EO, Codou A, Misra M, Mohanty AK. Materials today sustainability A critical review on the fabrication processes and performance of polyamide biocomposites from a biofiller perspective. Mater Today Sustain. 2019;5:100014. doi: 10.1016/j.mtsust.2019.100014.
(24) Oliver-Ortega H, Méndez JA, Espinach FX, Tarrés Q, Ardanuy M, Mutjé P. Impact strength and water uptake behaviors of fully biobased PA11-SGW composites. Polymers. 2018;10(7):1–12. doi: 10.3390/polym10070717.
(25) Alonso-Montemayor FJ, Tarrés Q, Oliver-Ortega H, Espinach FX, Narro-Céspedes RI, Castañeda-Facio AO, et al. Enhancing the mechanical performance of bleached hemp fibers reinforced polyamide 6 composites: A competitive alternative to commodity composites. Polymers. 2020;12(5):1041. doi: 10.3390/POLYM12051041.
(26) Singh R, Kumar R, Ranjan N. Sustainability of recycled ABS and PA6 by banana fiber reinforcement: thermal, mechanical and morphological properties. J Inst Eng (India): Ser C. 2019;100(2):351–60. doi: 10.1007/s40032-017-0435-1.
(27) Xu K, Zheng Z, Du G, Zhang Y, Wang Z, Zhong T, et al. Effects of polyamide 6 reinforcement on the compatibility of high-density polyethylene/environmental-friendly modified wood fiber composites. J Appl Polym Sci. 2019;136(38):16–8. doi: 10.1002/app.47984.
(28) Kunchimon SZ, Tausif M, Goswami P, Cheung V. Polyamide 6 and thermoplastic polyurethane recycled hybrid Fibres via twin-screw melt extrusion. J Polym Res. 2019;26(7):1–4. doi: 10.1007/s10965-019-1827-0.
(29) Aydemir D, Kiziltas A, Erbas Kiziltas E, Gardner DJ, Gunduz G. Heat treated wood-nylon 6 composites. Compos Part B: Eng. 2015;68:414–23. doi: 10.1016/j.compositesb.2014.08.040.
(30) Lods L, Richmond T, Dandurand J, Dantras E, Lacabanne C, Durand JM, et al. Thermal stability and mechanical behavior of technical bamboo fibers/bio-based polyamide composites. J Therm Anal Calorim. 2022;147(2):1097–106. doi: 10.1007/s10973-020-10445-z.
(31) Balla VK, Kate KH, Satyavolu J, Singh P, Tadimeti JGD. Additive manufacturing of natural fiber reinforced polymer composites: Processing and prospects. Compos Part B: Eng. 2019;174(March):106956. doi: 10.1016/j.compositesb.2019.106956.
(32) Nopparut A, Amornsakchai T. Influence of pineapple leaf fiber and it' s surface treatment on molecular orientation in, and mechanical properties of, injection molded nylon composites. Polym Test. 2016;52:141–9. doi: 10.1016/j.polymertesting.2016.04.012.
(33) Millot C, Fillot LA, Lame O, Sotta P, Seguela R. Assessment of polyamide-6 crystallinity by DSC: temperature dependence of the melting enthalpy. J Therm Anal Calorim. 2015;122:307–14.
(34) Salem IAS, Rozyanty AR, Betar BO, Adam T, Mohammed M, Mohammed AM. Study of the effect of surface treatment of kenaf fiber on chemical structure and water absorption of kenaf filled unsaturated polyester composite. J Phys: Conf Ser. 2017;908(1):012001. doi: 10.1088/1742-6596/908/1/012001.
(35) Nurazzi NM, Asyraf MRM, Rayung M, Norrrahim MNF, Shazleen SS, Rani MSA, et al. Thermogravimetric analysis properties of cellulosic natural fiber polymer composites: A review on influence of chemical treatments. Polymers. 2021;13(16):2710. doi: 10.3390/polym13162710.
(36) Şeker Hirçin B, Yörür H, Mengeloğlu F. Effects of filler type and content on the mechanical, morphological, and thermal properties of waste casting polyamide 6 (W-PA6G)-based wood plastic composites. BioResources. 2020;16(1):655–68. doi: 10.15376/biores.16.1.655-668.
(37) Kamarudin SH, Abdullah LC, Aung MM, Ratnam CT. Thermal and structural analysis of epoxidized jatropha oil and alkaline treated kenaf fiber reinforced poly(Lactic acid) biocomposites. Polymers. 2020;12(11):1–21. doi: 10.3390/polym12112604.
(38) Kiziltas EE, Yang HS, Kiziltas A, Boran S, Ozen E, Gardner DJ. Thermal analysis of polyamide 6 composites filled by natural fiber blend. BioResources. 2016;11(2):4758–69. doi: 10.15376/biores.11.2.4758-4769.
(39) Pereira PHF, Ornaghi HL, Arantes V, Cioffi MOH. Effect of chemical treatment of pineapple crown fiber in the production, chemical composition, crystalline structure, thermal stability and thermal degradation kinetic properties of cellulosic materials. Carbohydr Res. Nov 2020;499:108227. doi: 10.1016/j.carres.2020.108227.
(40) Cintra SC, Braga NF, Morgado GF, Montanheiro TL, Marini J, Passador FR, et al. Development of new biodegradable composites materials from polycaprolactone and wood flour. Wood Mater Sci Eng. 2021;17(6):586–97. doi: 10.1080/17480272.2021.1905712.
(41) Nagarajan V, Mohanty AK, Misra M. Perspective on polylactic acid (PLA) based sustainable materials for durable applications: focus on toughness and heat resistance. ACS Sustain Chem Eng. 2016;4(6):2899–916. doi: 10.1021/acssuschemeng.6b00321.

(42) Bhattacharjee S, Bajwa DS. Degradation in the mechanical and thermo-mechanical properties of natural fiber filled polymer composites due to recycling. Constr Build Mater. 2018;172:1–9. doi: 10.1016/j.conbuildmat.2018.03.010.
(43) Sridhara PK, Vilaseca F. Assessment of fiber orientation on the mechanical properties of PA6/Cellulose composite. Appl Sci (Switz). 2020;10(16):5565. doi: 10.3390/app10165565.
(44) García Hernández Z, Miranda Teran ZN, González Morones P, Yañez Macías R, Solís Rosales SG, Romero GY, et al. Performance of nylon 6 composites reinforced with modified agave fiber: Structural, morphological, and mechanical features. J Appl Polym Sci. 2021;138(34):1–11. doi: 10.1002/app.50857.
(45) Zhu R, Yadama V, Liu H, Lin RJT, Harper DP. Fabrication and characterization of Nylon 6/cellulose nanofibrils melt-spun nanocomposite filaments. Compos Part A: Appl Sci Manuf. 2017;97:111–9. doi: 10.1016/j.compositesa.2017.02.025.
(46) Zhu S, Guo Y, Chen Y, Liu S. Low water absorption, high-strength polyamide 6 composites blended with sustainable bamboo-based biochar. Nanomaterials. 2020;10(7):1–15. doi: 10.3390/nano10071367.
(47) Nematollahi M, Karevan M, Fallah M, Farzin M. Experimental and numerical study of the critical length of short Kenaf fiber reinforced polypropylene composites. Fibers Polym. 2020;21(4):821–8. doi: 10.1007/s12221-020-9600-x.
(48) Huzaifah MRM, Sapuan SM, Leman Z, Ishak MR. Effect of fibre loading on the physical, mechanical and thermal properties of sugar palm fibre reinforced vinyl ester composites. Fibers Polym. 2019;20(5):1077–84. doi: 10.1007/s12221-019-1040-0.
(49) Sridhara PK, Vilaseca F. High performance PA 6/cellulose nanocomposites in the interest of industrial scale melt processing. Polymers. 2021;13(9):1495. doi: 10.3390/polym13091495.
(50) Lee KW, Chung JW, Kwak SY. Highly branched polycaprolactone/glycidol copolymeric green plasticizer by one-pot solvent-free polymerization. ACS Sustain Chem Eng. 2018;6(7):9006–17.
(51) Renato Pereira de Melo. Development of polyamide composites with natural fibers for automotive applications. Materials. Ecole Nationale Supérieure des Mines de Paris; Universidade federal do Rio de Janeiro. 2015. English. ffNNT: 2015ENMP0062ff.
(52) Arjmandi R, Yıldırım I, Hatton F, Hassan A, Jefferies C, Mohamad Z, et al. Kenaf fibers reinforced unsaturated polyester composites: a review. J Eng Fibers Fabr. 2021;16:15589250211040184. doi: 10.1177/15589250211040184.
(53) Li S, Wang H, Chen C, Li X, Deng Q, Li D. Mechanical, electrical, and thermal properties of highly filled bamboo charcoal/ultra-high molecular weight polyethylene composites. Polym Compos. 2018;39:E1858–66. doi: 10.1002/pc.24839.
(54) Alonso-montemayor FJ, Tarr Q, Oliver-ortega H, Delgado-aguilar M. Enhancing the mechanical performance of bleached Hemp fibers reinforced polyamide 6 composites. Polymers. 2020;12:1041.